MICRO STRUCTURAL SNOWPACK PARAMETERS ASSOCIATED WITH FRACTURE CHARACTER IN COMPRESSION TESTS

Alec van Herwijnen, Sascha Bellaire and Jürg Schweizer
WSL, Swiss Federal Institute for Snow and Avalanche Research SLF, Davos, Switzerland

ABSTRACT: Compression tests are snow stability tests which are widely used by avalanche professional and snow researchers to identify potential weak snowpack layers. The test score, i.e. the loading step at the moment of failure, provides information about the strength of the weak layer. It therefore relates to fracture initiation, which is the first stage of avalanche release. The addition of a description of fracture character improves the interpretation of compression test results since certain types of fractures, i.e. sudden fractures, are more often associated with skier-triggered avalanches. Distinguishing between different types of fractures presumably provides information on fracture propagation, which is the second stage of avalanche release. The SnowMicroPen (SMP) was used to measure high resolution penetration resistance profiles. Using field data from over 100 such penetration resistance measurements observed in conjuncture with two compression tests, micro structural parameters associated with different types of fractures were identified. More than 300 fractures were classified as either Progressive Compression (2.2 %), Resistant Planar (7.6 %), Sudden Planar (60.3 %), Sudden Collapse (21.1 %) and non-planar Break (8.8 %). A method based on the autocorrelation of the signal was used to identify the failure layers (found with the compression tests) in the resistance profiles. Special attention was given to the micro structural properties of the failure layer, the layer adjacent to the failure layer and the slab above the failure layer. Sudden fractures were found to have typical micro structural snowpack parameters which are generally associated with unstable snow conditions, such as large differences in penetration resistance between the failure layer and the adjacent layer..

KEYWORDS: snow microstructure, snow mechanical properties, snow stability evaluation, stability test

1. INTRODUCTION

Snowpack data such as snow profiles and stability tests are often used for avalanche forecasting. The identification of potential weak layers within the snow cover is an important part of gathering these data and often relies on snow stability tests. The compression test is a snow stability test which is widely used by avalanche professional and snow researchers to identify these potential weak layers.

It is well known that the frequency of skier-triggered slab avalanches decreases with increasing test score (Jamieson, 1999). However, it is also well established that the test score can be highly variable and is not the only result relevant for stability evaluation. Additional information about the character of the fracture can provide valuable information (Johnson and Birkeland, 2002, van Herwijnen and Jamieson, 2007).

Corresponding author address: Alec van Herwijnen, WSL Institute for Snow and Avalanche Research SLF, Flüelastrasse 11, CH-7260 Davos Dorf, Switzerland;
tel: +41 81 4170175; fax: +41 81 4170110;
email: vanherwijnen@slf.ch

The test score, i.e. the loading step at the moment of failure, provides information about the strength of the weak layer. It therefore relates to fracture initiation, which is the first stage of avalanche release. The addition of a description of fracture character improves the interpretation of compression test results since certain types of fractures, i.e. sudden fractures, are more often associated with skier-triggered avalanches (van Herwijnen and Jamieson, 2007). Distinguishing between different types of fractures presumably provides information on fracture propagation, which is the second stage of avalanche release.

Previous research has shown that typical snowpack properties associated with sudden fractures favour skier-triggering, e.g. large hand hardness and crystal size differences between the failure layer and the adjacent layers (van Herwijnen and Jamieson, 2007). However, it is unclear why these snowpack properties favour sudden fractures since knowledge about the micro mechanism of the various fractures is largely unknown. In this study we analyse compression test results performed next to high resolution penetration resistance measurements of the snow cover. The goal is to identify typical micro structural snowpack parameters associated with different types of fractures in compression tests.

2. METHODS

2.1 Field measurements

As part of a study on spatial variability of snow stability we performed over 200 compression tests in 11 spatial grids around Davos, Switzerland, during the winters of 2006-2007 and 2007-2008 (Bellaire and Schweizer, 2008). Fractures in compression tests were systematically classified using a five level description of fracture character (van Herwijnen and Jamieson, 2007): Progressive Compression (PC), Resistant Planar (RP), Sudden Planar (SP), Sudden Collapse (SC) and non-planer Break (B).

In the centre of each spatial grid a manual snow profile was observed and two compression tests were performed. Two compression tests were also performed at 9 different locations throughout the grid in conjuncture with a SnowMicroPen (SMP) measurement (Figure 1). The SMP consists of a probe which is driven into the snow cover at a constant speed of 20 mm/s (Schneebeli and Johnson, 1998). A movable cone shaped tip with a diameter of 5 mm containing a piezo-electric force sensor records changes in hardness and snow structure. The force sensor measures penetration resistance approximately every 4 μm, i.e. 250 measurements per mm.

2.2 Snow surface detection

The first few cm of the SMP signal are recorded in the air as the tip of the probe moves towards the snow surface. In order to compare failure depths in the compression tests with layers within the SMP signal, an accurate detection of the snow surface is required. Usually, the snow-air interface is identified by hand, which is a time consuming endeavour. In order to automatically pick the snow surface, a signal processing method commonly used in seismology, the Akaike's Information Criterion (AIC), was applied to the SMP signal. The AIC function is based on the variance of the signal and is used to extract wave arrivals times (e.g. Kurz et al., 2005).

The AIC function gives reliable onset picks if the AIC is only applied to a part of the signal which contains the onset. Therefore, a rough estimate of the onset was determined by applying a simple threshold of 0.05 N to the moving averaged penetration resistance signal, averaged over 1000 measurements (approximately 4 mm). The global minimum in the AIC function of the raw SMP signal before the first crossing of the threshold determined the location of the snow surface.

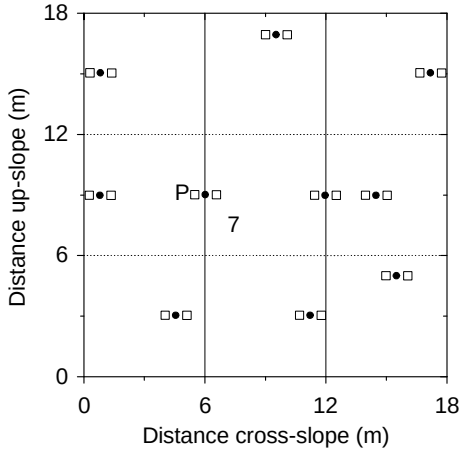

Figure 1: Schematic representation of spatial grid measurement layout. The location of the manual profile is indicated with a P, SMP measurements by full circles and compression tests by open squares.

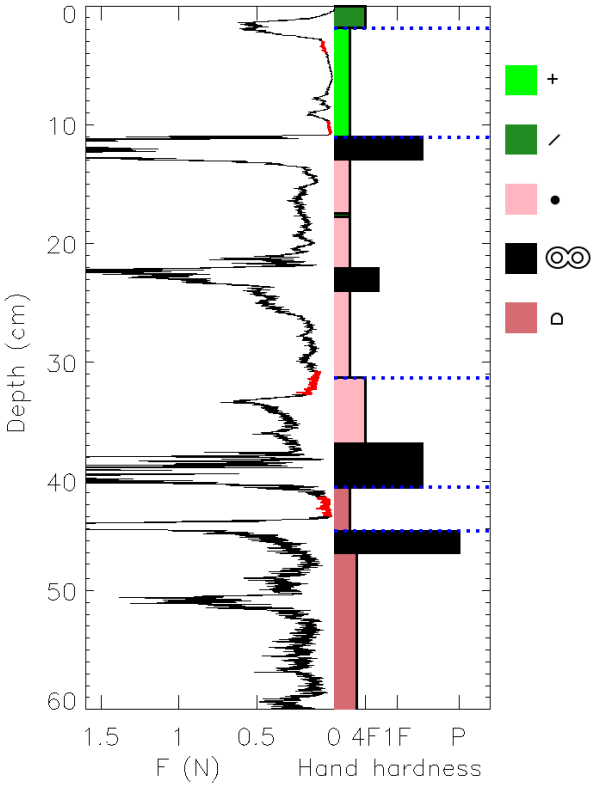

Figure 2: Manual picking of failure layers in the SMP signal was done in the SMP signal next to the manual snow profile. (left) SMP signal. (right) Hand hardness and crystal type of manual snow profile. The blue dashed lines indicate failures in compression tests and the red portions of the SMP signal the manually picked failure layers.

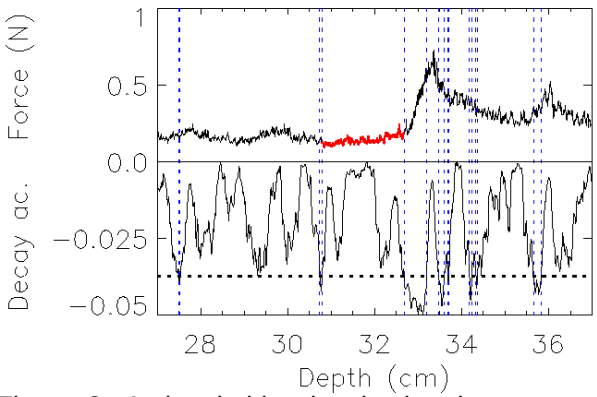

Figure 3: A threshold value in the decay was manually picked to isolate the part of the signal coinciding with the failure layer. (top) SMP signal and failure layer (red). (bottom) Decay in the autocorrelation function and threshold value (black dashed line). The blue dashed vertical lines indicate picked layer boundaries.

2.3 Failure layer detection

SMP measurements have so far mainly been used to study the micro mechanical properties of known failure layers. Their location in the SMP signal was identified by hand based on an adjacent manual snow profile. However, if the location of the failure layer in the SMP profile is largely unknown, for example, when no manual snow profile is available, the identification of failure layers is not straightforward since failure layers can be relatively thick and not much weaker than the surrounding snow.

Failure layers in compression tests were therefore first identified within the manually observed snow profile, which served as a reference. By comparing the snow profile with the SMP signal measured next to it the failure layers were manually identified within this SMP signal (Figure 2). By matching the SMP signal with the manually identified failure layers to the remaining SMP signals, i.e. those 9 measurements not close the profile location, a method was developed to automatically pick the failure layer. This method proceeds in the following way:

1. Mean SMP signals, denoted by S, were generated at each measurement location by taking the average over 25 points, corresponding to approximately 0.1 mm.
2. The decay of a moving window autocorrelation was determined for a 10 cm long section of the mean SMP signal ($S_{p,FL}$) centred around the middle of the manually identified failure layer at the profile location. The autocorrelation is a mathematical method for finding repeating patterns within a signal by correlating the signal with a shifted version of itself. A correlation coefficient is calculated for different shift distances, called lags. The decay in the correlation coefficient with lag distance indicates whether the signal is spatially homogeneous or not. The idea behind using this method is that the decay of the autocorrelation should be relatively low within the failure layer and should increase at the interface with the adjacent layers. At every data point along $S_{p,FL}$ the exponential decay of the moving window autocorrelation was calculated for windows of 50 points (i.e. 5 mm

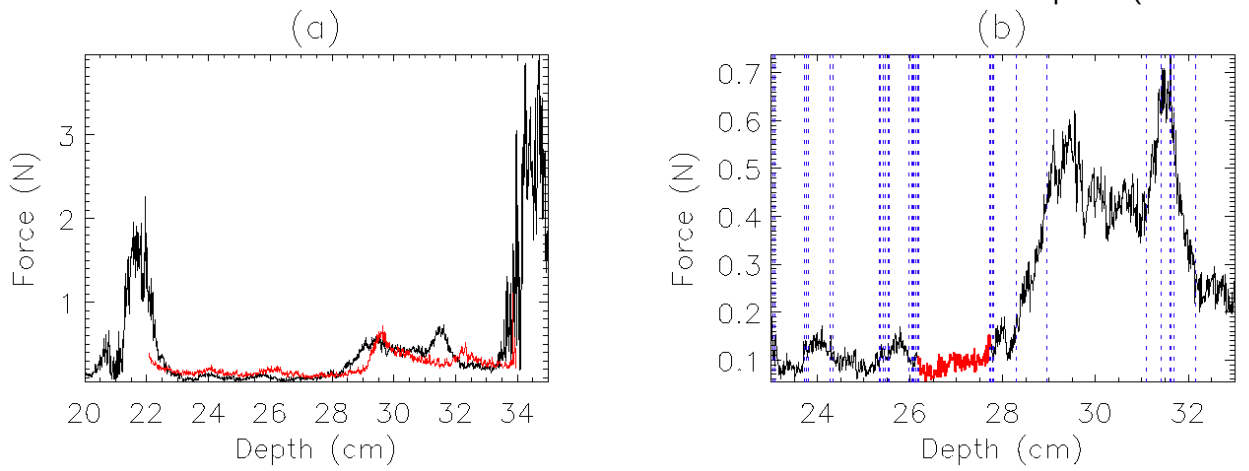

Figure 4: (a) Best match between a SMP signal not taken at the profile location and the signal containing the manually picked failure layer from the profile location. (b) Automatic failure layer detection (red portion of the signal) based on the decay of the autocorrelation. Blue dashed lines indicate layer boundaries.

windows). A threshold value in the decay was manually picked to isolate the part of the signal coinciding with the failure layer (Figure 3).

3. A rough localization of the failure layer within the other SMP signals was obtained by cross-correlating $S_{p,FL}$ with the mean SMP signal at the other locations in the grid. This was done by searching for a global maximum in the cross-correlation of $S_{p,FL}$ with a 20 cm portion of the SMP signals centred around the depth of the failure layer in the compression test at the different locations (Figure 4a).
4. The exact location of the failure layer was determined using the decay of the moving window autocorrelation of the portion of the signal which most closely matched $S_{p,FL}$. By using the same threshold value for the decay of the autocorrelation as determined at the profile location, the failure layer was automatically identified within the SMP signal (Figure 4b).

In order to use this method only failures in compression tests that were linked to layers observed in the snow profile could be used in the analysis, excluding 43 from the 361 recorded fractures. In 87% of the cases the failure layer was picked at the right location. In the remaining 13% of the cases the automatically picked failure layer was not in the right location because the cross-correlated signals were not matched adequately. In these cases the best match between the SMP signals was manually determined and the exact location of the failure layer was picked using the method described above.

2.4 Adjacent layer detection

The location of the layer adjacent to the failure layer, either the layer above or the layer below the failure layer, was determined by examination of the fracture in the compression test and identified within the manual snow profile. Automatic detection of these layers within the SMP profiles using the method described above was not satisfactory. This was mainly because most adjacent layers were relatively hard (e.g. windslab or melt-freeze crust) corresponding to a more noisy signal (i.e low autocorrelation). Furthermore, there was more variability in the adjacent layers than in the failure layers, severely reducing the accuracy of the layer matching by cross-correlation. Therefore, the layers adjacent to the failure layers were identified manually within each SMP profile.

The slab above the weak layer was chosen as all layers above the failure layer. When the fracture in the compression test occurred at the top of the failure layer, the layer adjacent to the failure layer was included in the slab.

Table 1: Micro structural parameters derived from the penetration resistance measurement

Parameter	Description
$\overline{F}$ (N)	Mean penetration resistance
n_{peaks} (mm^{-1})	Number of ruptures per mm
L_n (mm)	Element length
f_r (N)	Rupture force
E (kPa)	Macro mechanical elastic modulus
Σ (kPa)	Macro mechanical compactive strength
Ψ (kPa)	Structural parameter

2.5 Micro structural SMP parameters

Johnson and Schneebeli (1999) developed a micro structural model to derive micro mechanical properties of snow layers from the SMP signal. The micro structural parameters which were extracted from the signal are given in Table 1 (for a more detailed description of these parameters see Bellaire and Schweizer, 2008). The structural parameter ψ is the product of the number of fractures per mm and the rupture force divided by the area of the SMP tip (Bellaire et al., 2008). The mean values of these parameters were derived for the failure layer (FL), the adjacent layer (AL) and for the slab (SL). Furthermore, relative differences in these parameters, denoted by Δ, between the failure layer and both the adjacent layer and the slab were calculated. For instance, the relative difference in mean force between the slab and the failure layer was calculated as:

$$\Delta\overline{F}_{SL-FL} = \frac{\overline{F}_{SL} - \overline{F}_{FL}}{\overline{F}_{SL}} . \quad (1)$$

2.6 Statistical comparison

Non parametric descriptors, e.g. median rather than mean, were used to characterize the distributions since the SMP signal is generally non-normally distributed. To compare data we used the non-parametric Mann-Whitney *U*-test. Since Sudden Planar fractures were most common in our data set, we used these as a reference to compare data from other fracture types with. Data were considered significantly different for $p \leq 0.01$.

Table 3: Number of observations and frequency of observation for each category of fracture character

Frac. char.	*N*	Freq. of obs. (%)
PC	7	2.2
RP	24	7.6
SP	192	60.3
SC	67	21.1
B	28	8.8

3. RESULTS

The frequency of observation for each fracture type is given in Table 1. SP fractures were most often observed, followed by SC, B RP and PC fractures. There were only 7 recorded PC fractures in our data. Previous work has shown that PC and RP fractures are typically associated with similar snowpack conditions (van Herwijnen and Jamieson, 2007). Therefore, we decided to group both fractures in one category.

3.1 Layer properties

The results from the statistical comparison of micro structural parameters and fracture character for the failure layer, the adjacent layer and the slab are shown in Table 3.

The micro structural parameters associated with non-planer Breaks (B) showed no significant difference with those from SP fractures. On the other hand, most all parameters associated with PC and RP fractures were significantly different from SP fractures. Failure layers, adjacent layers and slabs associated with PC/RP fractures generally had lower penetration resistance, rupture force, elastic modulus, compressive strength and structural parameter. The element length on the other hand was significantly larger, which was also

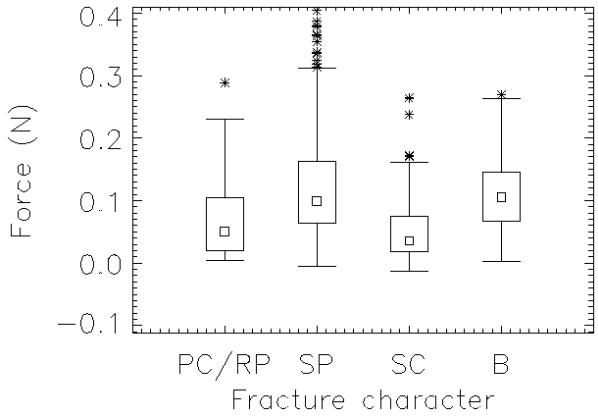

Figure 5: Distribution of mean penetration resistance of the failure layer for each fracture type. The squares indicate the median value, the boxes indicate the interquartile range and the whiskers show the largest non-outlier range. The outliers are shown by asterisks.

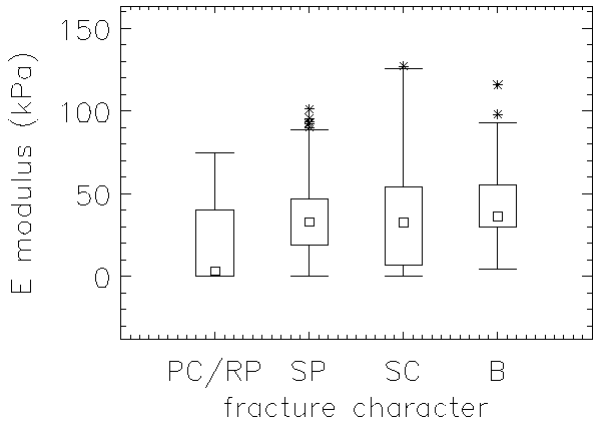

Figure 6: Distribution of the mean macro mechanical elastic modulus of the slab for each fracture character. Symbols as in Figure 5.

Table 2: Median values of the penetration resistance $\bar{F}$, number of ruptures per mm n_{peaks}, element length L_n, rupture force f_r, elastic modulus E, compressive strength Σ and structural parameter Ψ for each fracture type. Variables that were significantly different from SP are marked in bold.

	Failure layer				Adjacent layer				Slab			
Para.	SP	SC	B	PC/RP	SP	SC	B	PC/RP	SP	SC	B	PC/RP
$\bar{F}$	0.10	**0.04**	0.10	**0.05**	0.5	0.37	0.52	**0.13**	0.26	0.20	0.33	**0.14**
n_{peaks}	15.5	**4.0**	16.6	8.2	34.5	**22.6**	36.9	**12.7**	16.4	**8.8**	18.5	**3.9**
L_n	1.3	**2.1**	1.3	**1.7**	0.9	**1.1**	0.9	**1.4**	1.2	**1.4**	1.2	**2.0**
f_r	0.04	0.03	0.04	**0.02**	0.07	0.09	0.06	**0.04**	0.07	0.06	0.07	**0.03**
E	13.1	**5.1**	14.4	**3.6**	60.0	68.5	53.1	**12.7**	33.0	32.6	36.4	**3.4**
Σ	1.3	1.1	1.4	**0.8**	2.9	3.9	2.4	**1.2**	1.7	1.8	1.7	**1.0**
Ψ	13.5	**2.9**	14.6	**2.8**	66.2	60.1	52.4	**10.4**	29.5	23.0	35.6	**2.2**

the case for SC fractures.

The distributions of the mean penetration resistance of the failure layer are shown in Figure 5, while the distribution of the elastic modulus of the slab is shown in Figure 6. Clearly PC/RP fractures and SC fractures were associated with failure layers with a lower penetration resistance. As seen in Figure 6, slabs associated with PC/RP fractures had a lower elastic modulus than slabs associated with other fracture types. Furthermore, the median value of E_{SL} was somewhat higher for from B than for SP and SC.

3.2 Relative layer properties

The results from the statistical comparison of micro structural parameters and fracture character for the relative difference between the adjacent layer and the failure layer as well as between the slab and the failure layer are shown in Table 4. Again, no significant differences were observed between SP and B fractures, while both SC and PC/RP fractures had parameters significantly different from SP fractures. Compared to SP fractures, failure layers associated with SC fractures exhibited larger relative differences in hand hardness, number of fractures per mm, elements length, elastic modulus and structural parameter. PC/RP fractures on the other hand were associated with significantly smaller Δn_{peaks}, ΔL_n and $\Delta \Psi$ than SP fractures.

Table 4: Median values of relative differences of micros structural parameters between the adjacent layer and the failure layer as well as between the slab and the failure layer. Variables that were significantly different from SP are marked in bold.

	Adjacent layer and failure layer			
Para.	SP	SC	B	PC/RP
$\Delta \overline{F}_{AL\text{-}FL}$	0.80	**0.91**	0.81	0.81
$\Delta n_{peaks\ AL\text{-}FL}$	0.52	**0.82**	0.52	**0.31**
$\Delta L_{n\ FL\text{-}AL}$	0.27	**0.46**	0.26	**0.19**
$\Delta f_{r\ AL\text{-}FL}$	0.38	0.49	0.30	0.52
$\Delta E_{AL\text{-}FL}$	0.69	**0.91**	0.60	0.60
$\Delta \Sigma_{AL\text{-}FL}$	0.39	0.47	0.29	0.51
$\Delta \Psi_{AL\text{-}FL}$	0.51	**0.77**	0.57	**-0.23**
	Slab and failure layer			
$\Delta \overline{F}_{SL\text{-}FL}$	0.64	**0.74**	0.69	0.57
$\Delta n_{peaks\ SL\text{-}FL}$	0.21	**0.59**	0.14	**-0.93**
$\Delta L_{n\ FL\text{-}SL}$	0.12	**0.23**	0.09	**-0.26**
$\Delta f_{r\ SL\text{-}FL}$	0.35	0.33	0.57	0.48
$\Delta E_{SL\text{-}FL}$	0.48	**0.69**	0.54	**-0.02**
$\Delta \Sigma_{SL\text{-}FL}$	0.09	0.13	0.29	0.32
$\Delta \Psi_{SL\text{-}FL}$	0.51	**0.77**	0.57	**-0.23**

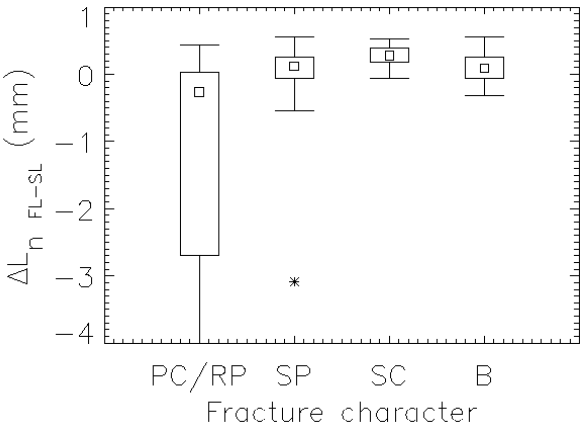

Figure 7: Distribution of the relative difference in element length between the failure layer and the slab for each fracture type. Symbols as in Figure 5.

The distribution of the relative difference in structural length between the slab and the adjacent layer is shown in Figure 7.

4. DISCUSSION AND CONCLUSIONS

The method used to determine the snow surface was fast and effective. It can reliably be used to determine the snow surface in high quality signals. However, when the signal-to-noise ratio of the signal in the air increases, e.g. due to signal drift, the snow surface is not accurately picked. Manual picking of the snow surface is then still required.

Using the autocorrelation of the signal to automatically identify failure layers within the signal was relatively successful. However, it required the manual picking of a reference layer from the SMP signal measured at the location of the manually observed snow profile. Nonetheless, while further development is required, such a method could potentially be used to automatically identify layer boundaries within SMP signals, which would greatly improve and facilitate the analysis and interpretation of SMP signals.

The data analysed here were collected for a study on spatial variability of snow stability. Even though there were over 300 recorded fractures, the data were only collected on 11 individual days. Therefore, snowpack conditions were not very diverse. Nevertheless, the statistical comparison of micro structural parameters associated with fracture character revealed interesting differences.

Field measurements of hand hardness can be thought of a rough penetration resistance measurement, while crystal size can be related to

element length. Regarded in such a manner, the typical micro structural snowpack parameters associated with fracture character (Table 3 and 4) closely relate to typical manual snow profile parameters associated with fracture character (van Herwijnen and Jamieson, 2007). For instance, PC and RP fractures were typically associated with soft new snow layers which explains the low penetration resistance and larger element size. Furthermore, the differences in hardness and crystal size were typically small, i.e. small relative differences in penetration resistance and element length. SP and SC fractures on the other hand were generally associated with larger differences in hand hardness and crystal size, in good agreement with the relative differences in element length and penetration resistance (Table 4), although the differences were not as pronounced. Finally, manual snowpack parameters for SP and B fractures were often similar, which was also the case in the present study.

A study on the micro structural parameters associated with stable and unstable snow profiles (Pielmeier et al., 2007) revealed that unstable snowpack layers typically have a low mean penetration resistance, significantly lower than the adjacent layer. Furthermore, unstable snowpack layers generally have a large mean element length and a low number of ruptures, significantly lower than the adjacent layer. The results presented in the study confirm that sudden fractures have typical micro structural snowpack parameters which are generally associated with unstable snow conditions (Table 6 and 7). However, B fractures, which are typically not associated with skier-triggering, were also associated with these micro-structural parameters. Therefore, it is crucial that more data with a wider range of snowpack conditions will be collected and analysed to determine the validity of the findings presented here.

ACKNOWLEDGEMENTS

For their careful field work and tireless digging we would like to thank Christoph Mitterer, Sina Schneider, Michael Schirmer, Charles Fierz and Martin Schneebeli. Thanks to Henning Loewe, Chris Pielmeier and Martin Schneebeli for stimulating discussions.

REFERENCES

Bellaire, S. and J. Schweizer, 2008: Deriving spatial stability variations from penetration resistance measurements. *Proceedings ISSW 2008, International Snow Science Workshop, Whistler, Canada, 21-27 September 2008*, this proceedings.

Bellaire, S., C. Pielmeier, M. Schneebeli, and J. Schweizer, 2008: Stability algorithm for snow micro-penetrometer measurements. *J. Glaciol.*, submitted.

Jamieson, J. B., 1999: The compression test - after 25 years. *The Avalanche Review*, **18**(1), 10-12.

Johnson, R.F. and K.W. Birkeland, 2002: Integrating shear quality into stability test results. *Proceedings ISSW 2002, International Snow Science Workshop, Penticton BC, Canada, 29 September-4 October 2002*, International Snow Science Workshop Canada Inc., BC Ministry of Transportation, Snow Avalanche Programs, Victoria BC, Canada, 508-513.

Johnson, J.B. and M. Schneebeli, 1999: Characterizing the microstructural and micromechanical properties of snow. *Cold Reg. Sci. Technol.*, **30**(1-3), 91-100.

Kurz, J.H., C.U. Grosse and H.W. Reinhardt, 2005: Strategies for reliable automatic onset time picking of acoustic emissions and of ultrasound signals in concrete. *Ultrasonics*, **43**, 538-546.

Pielmeier, C. and J. Schweizer, 2007: Snowpack stability information derived from the SnowMicroPen. *Cold Reg. Sci. Technol.*, **47**(1-2), 102-107.

Schneebeli, M. and J.B. Johnson, 1998: A constant-speed penetrometer for high-resolution snow stratigraphy. *Ann. Glaciol.*, **26**, 107-111.

van Herwijnen, A. and Jamieson, B., 2007. Fracture character in compression tests. *Cold Reg. Sci. Technol.*, **47**(1-2), 60-68.